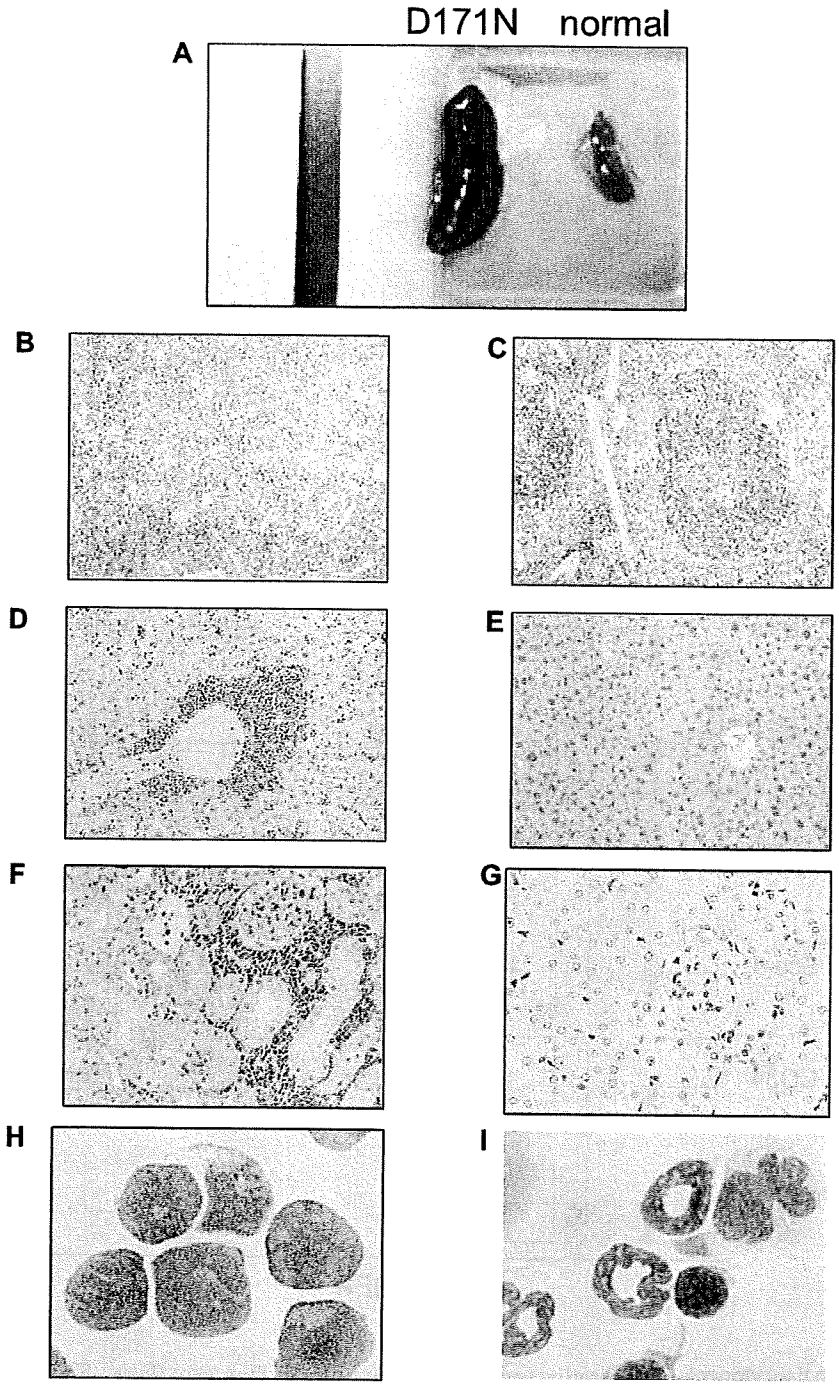

Figure 6. Leukemic cells of mice/D171N with high expression of Evi1 invaded into liver and kidney. (A) Spleen from morbid mice/D171N (left) and from normal mice (right). Histopathologic findings of (B) spleen, (D) liver, and (F) kidney infiltrated with leukemic cells from mice/D171N, stained with H&E. Histopathologic findings of (C) spleen, (E) liver, and (G) kidney from normal mice, stained with H&E. (H) Mice/D171N showed a high percentage of blasts in bone marrow. Cytospin preparations of BM cells from (H) mice/D171N and (I) normal mice, stained with Giemsa. (BX51 microscope, DP12 camera module; objective lens, UPlanFl; magnification, ×200 (B-E); ×100 (F,G); and ×1000 (H,I).

although previous studies either using similar BMT models or knock-in mice of *AML1* mutants failed to do so. There are several potential explanations for this discrepancy. First, because most *AML1* mutants work as dominant-negative forms, high expression levels of the mutants would be critical to effectively inhibit WT *AML1*. In this aspect, our BMT model has an advantage, using the efficient retrovirus vector pMYs[40] designed to achieve high expression in hematopoietic progenitor cells and, unlike most other retrovirus vectors, harbors splice donor and acceptor sites derived from the MFG vector to increase expression levels.[40,47] Second, using the efficient packaging cell line Plat-E,[39] we achieved high titers of retroviruses (average: 10^7 infection U/mL), which could result in the higher numbers of retrovirus integrations. This also increases the probabilities of up-regulating or disrupting important genes that collaborate with *AML1* mutants in inducing MDS and/or MDS/AML. Alternatively, it is also possible that the positions of *AML1* mutations are critical for the biological effect. We believe that the combination of these factors has put our system into practice.

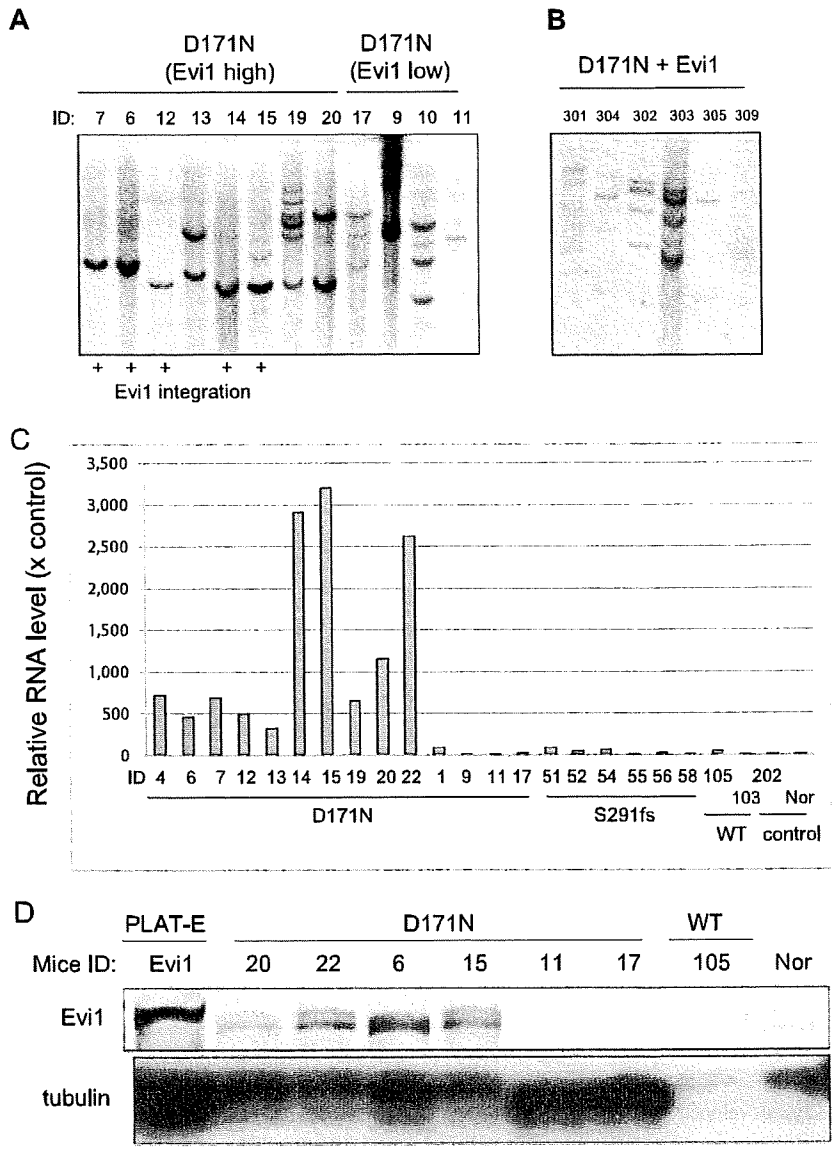

Figure 7. The mice/D171N with integration near *Evi1* site were monoclonal. (A) Southern blot analysis of mice/D171N. DNA samples were digested with *Eco*RI, which cut the retrovirus only once within the multicloning site. Probes used were DNA fragments of the GFP coding sequence. Mouse IDs are shown at the top of the panel. (B) The mice/D171N + *Evi1* were polyclonal. DNA samples were digested with *Eco*RI. Proviruses were probed with a GFP probe. (C) Real-time PCR for *Evi1* in BM derived from morbid mice/D171N or mice/S291fs or mice/WT or mice/mock. In addition to 6 samples from mice/D171N harboring integration near *Evi1* (mouse IDs 4, 6, 7, 12, 14, and 15), 4 samples derived from mice/D171N without integration near *Evi1* display high expression levels of Evi1 (mouse IDs 13, 19, 20, and 22). RNA from normal BM cells served as a control (RNA level = 1). (D) Western blot of lysates from spleen cells of mice/D171N, mice/WT, and normal mice and PLAT-E as controls. Samples from mice/D171N confirmed high expression of *Evi1* by RT-PCR showed expression of the protein (mouse IDs 6, 15, 20, and 22), but the other mice without high expression of *Evi1* by RT-PCR did not express the protein (mouse IDs 11, 17, and 105).

In the present MDS model, we used 2 *AML1* mutants, D171N and S291fsX300. The latter, a C-terminal–truncated form, is more potent as a dominant-negative form than the former, which harbors a point mutation in the RHD.[25,26] In this context, it is reasonable that the S291fs mutant induced the disease in the mice that underwent transplantation with a higher penetrance (Figure 1D). More important, expression of these mutants induced MDS/AML of distinct phenotypes in the mice that underwent transplantation: AML1-S291fs induced pancytopenia associated with dysplasia in the erythroid lineage, while AML1-D171N frequently induced hepatoslenomegaly and leukocytosis associated with marked myeloid dysplasia. This suggests that even different mutations of the same gene could induce heterogeneous diseases. As previously described,[25,26] AML1-D171N lost DNA-binding ability and hence transactivation potential because it possessed a point mutation in RHD essential for DNA-binding, while AML1-S291fs had increased DNA-binding ability but lost transactivation potential because it had an intact RHD but lacked a C-terminal transactivation domain. Thus, the different biological outcomes induced by *AML1* mutants could be explained in part by structural and functional differences between the mutants. In addition to the dominant-negative functions, these mutants may also have gain of function; the fact that AML1-KO mice did not develop leukemia[18] indicates that deletion of *AML1* alone is not sufficient to induce leukemia, suggesting the possibility that the *AML1* mutants have gain of function as well. Because *AML1* associates and forms a ternary complex with other transcriptional factors and cofactors via its specific domains, it is possible that these mutants exert different effects on the proliferation and differentiation of BM cells in the various contexts.

In BMT models using retrovirus-mediated gene transfer, the genes near the retrovirus integration sites are thought to affect the outcomes.[30-38] This sometimes obscures the significance of the transduced gene, but simultaneously will give us clues to understanding the collaboration of multiple genes in the development of leukemias. One of the intriguing findings of the present work is that high expression of *Evi1*, either caused by virus integration or by unknown mechanisms, was able to collaborate with AML1-D171N in inducing the homogeneous disease characterized by leukocytosis, severe myelodysplasia, and marked hepatosplenomegaly that

Table 1. Analysis of integration site

Mutant	Mouse ID	Count of Southern blot bands	Nearest gene	Chromosome no.	Gene ID	Distance to gene (start or end), bp	Location	Forward or reverse orientation	RTCGD hits
Experiment 1									
D171N	1	ND	*2010111I01Rik*	13	72061	238 927	Intron 10	F	0
D171N	1		*LOC100040862*	12	100040862	40 051	5′	F	0
D171N	4	ND	*Evi1*	3	14013	107 412	5′	R	24
D171N	4		*Nsmce2*	15	68501	221 183	Intron 5	R	2
Experiment 2									
D171N	5	3	*Rreb1*	13	68750	14 071	5′	R	9
D171N	5		*LOC619665*	6	619665	123 854	5′	F	0
D171N	6	1	*Evi1*	3	14013	106 286	5′	R	24
D171N	7	1	*Evi1*	3	14013	106 286	5′	R	24
Experiment 3									
D171N	10	4	*B4galt6*	18	56386	8 961	Intron 1	R	0
D171N	11	2	*Rp1h*	1	19888	65 523	5′	F	0
Experiment 4									
D171N	12	1	*Evi1*	3	14013	14 909	5′	F	24
D171N	13	2	*Slc38a2*	15	67760	41 018	5′	F	6
D171N	14	1	*Evi1*	3	14013	15 002	5′	F	24
D171N	15	2	*Evi1*	3	14013	14 850	5′	F	24
D171N	15		*Slc38a2*	15	22462	11 988	5′	R	6
S291fsX300	51	ND	*LOC100042800*	13	100042800	27 734	5′	R	0
S291fsX300	52	2	*P2rx7*	5	18439	40 672	Intron 13	R	1
S291fsX300	52		*Gm pr2*	14	105446	17	Intron 1	R	0
S291fsX300	54	2	*M srb3*	10	320183	98 981	3′	F	0
Empty	203	ND	*Dph5*	3	13609	70 064	5′	R	1
Experiment 5									
D171N	19	6	*Gch1*	14	14528	16 958	Intron 1	R	0
D171N	20	2	*Gch1*	14	14528	16 958	Intron 1	R	0
S291fsX300	55	2	*Mn1*	5	433938	16 024	Intron 1	F	8
S291fsX300	56	1	*Mn1*	5	433938	16 024	Intron 1	F	8
S291fsX300	58	1	*Mn1*	5	433938	16 024	Intron 1	F	8
Experiment 6									
D171N	22	ND	*Lrrc8c*	5	100604	16 056	5′	F	4
Experiment 7									
D171N	26	1	*Evi1*	3	14013	106 710	5′	F	24
S291fsX300	60	3	*Dock10*	1	210293	163 158	Intron 1	R	0

RTGCD, Retroviral Tagged Cancer Gene Database[37]; and ND, not determined.

always developed to overt leukemia with high percentages of $B220^+$ and $CD11b^+$ blasts. Together with the recent findings that Evi1 expression was observed in patients with MDS and AML,[36,48] and that Evi1 alone did not induce AML in mouse models,[14,34,49,50] our result strongly suggested that AML1-D171N collaborated with Evi1 in inducing MDS/AML. It is interesting to note that AML1-S291fs never collaborated with *Evi1* during our examination (Table 1), again suggesting that these 2 *AML1* mutations transform hematopoietic cells through distinct mechanisms. Importantly, we confirmed the collaboration between AML1-D171N and *Evi1* in an in vivo experiment. Cotransduction of AML1-D171N and *Evi1* into BM cells resulted in rapid induction of MDS/AML in the mice that received transplants. In addition, the leukemic cells in most of these mice included more clones than those in mice/D171N (Figure 7B), indicating cooperation of *Evi1* and AML1-D171N. However, leukemic cells from one mouse (ID 305) seemed to be monoclonal and to contribute to oligoclonal leukemia of mouse 304. In addition, it took 2 to 3 months for leukemias induced by the combination of AML1-D171N and Evi1 to kill the mice that received transplants. Together, these result suggested that while AML1-D171N and Evi1 overexpression collaborated in inducing leukemia, additional steps were required for efficient transformation of hematopoietic progenitors. In the absence of Evi1 high expression, AML1-D171N caused MDS or MDS/AML with low percentages of blasts in BM but still with hepatosplenomegaly. This indicates that hepatosplenomegaly had something to do with AML1-D171N.

In contrast to mice/D171N, most mice/S291fs succumbed to either MDS-RAEB with fatal severe anemia following continuous pancytopenia or MDS/AML without leukocytosis. The integration site in the intron 1 of the *MN1* gene found in leukemic cells of 3 mice was derived from the same cell. We also found that *MN1* was overexpressed in the leukemic cells of these mice, suggesting that overexpression of *MN1* induced effective expansion of leukemic stem cells. Recently, Heuser et al reported that high expression of *MN1* correlated with poor outcome in AML with normal cytogenetics.[51] Moreover, Slape et al identified *MN1* as potential collaborators of NUP98/HOXD13 to induce leukemia.[42] Further work will be required to investigate the role of MN1 in MDS/AML.

One fundamental question of this study was whether *AML1* mutants alone induce MDS and MDS/AML. In our experiments, 5 of the 6 surviving mice/D171N showed a disappearance of GFP^+ cells in time, suggesting that AML1-D171N alone was not able to induce MDS/AML. Previous studies using gene-engineered mice and a BMT model demonstrated that *AML1*

fusions caused by chromosomal translocations alone were insufficient to induce AML,[7-12] except for *AML1-MDS1-Evi1*, which by itself induced AML with a long latency.[52] In addition, several lines of evidence[30-38] that implicated the integration site of retroviruses for different biological outcomes led us to consider the same possibility in this BMT model. Indeed, we identified frequent retrovirus integrations near the *Evi1* gene in the BM cells derived from mice/D171N whose leukemic cells displayed nearly identical phenotypes and concomitant elevated expression of *Evi1*. Importantly, coexpression of AML1-D171N and *Evi1* induced the same leukemia with shorther latencies, demonstrating the collaboration between AML1-D171N and *Evi1* in vivo. These results showed the power of in vivo insertional mutagenesis of retroviruses in a search for genes involved in the pathogenesis of MDS and MDS/AML.

Finally, it is important to relate these in vivo results to clinical data of the human disease. The recent finding[25-27] that *AML1* point mutations in the C-terminal regions were almost exclusively found in MDS-RAEB and MDS/AML, but not in de novo AML, coincided with our data that AML1-S291fs tended to induce MDS-RAEB–like symptoms in this BMT model. Clinical findings[25-27] that the RHD point mutation was often found in de novo AML, mainly AML M0, in addition to MDS-RAEB and MDS/AML, was also in accordance with our data that AML1-D171N induced more progressive MDS/AML with higher percentages of blasts when compared with AML1-S291fs. Classification of MDS and MDS/AML is always controversial because of the heterogeneity of the disease.[1,2,27] In the future, this disease will be reclassified based on genetic alterations and their combinations.

In summary, we have generated a mouse BMT model of MDS-RAEB and MDS/AML. The current BMT model, mimicking AML1-related MDS, will be useful for understanding molecular pathogenesis and establishing new therapeutic strategy for MDS and MDS/AML.

Acknowledgments

We greatly thank Dr Mineo Kurokawa for kindly providing the anti-*Evi1* antibody and Dr Takuro Nakamura and Dr Kazuhiro Morishita for kindly providing pMYs-*Evi1*-IG. We also thank Dr Christopher Slape for kindly giving information about the condition of RT-PCR for MN1. We are grateful to Dr Dovie Wylie for excellent language assistance. We thank Yumi Fukuchi, Fumi Shibata, Miyuki Ito, and Ai Hishiya for technical assistance.

This work was supported by the Grant-in-aid for Cancer Research supported by the Ministry of Health, Labor and Welfare, Japan; a grant from the Vehicle Racing Commemorative Foundation; and a grant from the Japan Society for the Promotion of Science (JSPS). N.W.-O. is a JSPS research fellow.

Authorship

Contributions: N.W.O. did all the experiments and participated in writing the manuscript; J.K. oversaw all the experiments and actively participated in manuscript writing; R.O. provided experimental guidance about and assisted in the BMT model; H.H. provided the general information and made the constructs of AML1 mutants; Y.H. made the constructs of AML1 mutants; Y.K. assisted in the experiments of BMT model; H.N. provided experimental guidance about cell sorting and staining; T.N. provided experimental guidance of the BMT model; T.I. provided the general information and constructs of AML1 mutants; and T.K. conceived and directed the project, secured funding, and actively participated in manuscript writing.

Conflict-of-interest disclosure: The authors declare no competing financial interests.

Correspondence: Toshio Kitamura, Division of Cellular Therapy, Advanced Clinical Research Center, The Institute of Medical Science, The University of Tokyo, 4-6-1 Shirokanedai, Minato-ku, Tokyo 108-8639, Japan; e-mail: kitamura@ims.u-tokyo.ac.jp.

References

1. Mufti G, List AF, Gore SD, Ho AY. Myelodysplastic syndrome. Am Soc Hematol Educ Program. 2003;176-199.
2. Heaney ML, Golde DW. Myelodysplasia. N Engl J Med. 1999;340:1649-1660.
3. Legare RD, Gilliland DG. Myelodysplastic syndrome. Curr Opin Hematol. 1995;2:283-292.
4. Hirai H, Kobayashi Y, Mano H, et al. A point mutation at codon 13 of the N-ras oncogene in myelodysplastic syndrome. Nature. 1987;327:430-432.
5. Hirai H, Okada M, Mizoguchi H, et al. Relationship between an activated N-ras oncogene and chromosomal abnormality during leukemic progression myelodysplastic syndrome. Blood. 1988; 71:256-258.
6. Gilliland DG, Griffin JD. Role of FLT3 in leukemia. Curr Opin Hematol. 2002;9:274-281.
7. Schessl C, Rawat VP, Cusan M, et al. The AML1-ETO fusion gene and the FLT3 length mutation collaborate in inducing acute leukemia in mice. J Clin Invest. 2005;115:2159-2168.
8. Okuda T, Cai Z, Yang S, et al. Expression of a knocked-in AML1-ETO leukemia gene inhibits the establishment of normal definitive hematopoiesis and directly generates dysplastic hematopoietic progenitors. Blood. 1998;91:3134-3143.
9. Rhoades KL, Hetherington CJ, Harakawa N, et al. Analysis of the role of AML1-ETO in leukemogenesis, using an inducible transgenic mouse model. Blood. 2000;96:2108-2115.
10. Higuchi M, O'Brien D, Kumaravelu P, Lenny N, Yeoh EJ, Downing JR. Expression of a conditional AML1-ETO oncogene bypasses embryonic lethality and establishes a murine model of human t(8;21) acute myeloid leukemia. Cancer Cell. 2002;1:63-74.
11. Fenske TS, Pengue G, Mathews V, et al. Stem cell expression of the AML1/ETO fusion protein induces a myeloproliferative disorder in mice. Proc Natl Acad Sci U S A. 2004;101:15184-15189.
12. de Guzman CG, Warren AJ, Zhang Z, et al. Hematopoietic stem cell expansion and distinct myeloid developmental abnormalities in a murine model of the AML1-ETO translocation. Mol Cell Biol. 2002;22:5506-5517.
13. Ono R, Nakajima H, Ozaki K, et al. Dimerization of MLL fusion proteins and FLT3 activation synergize to induce multiple-lineage leukemogenesis. J Clin Invest. 2005;115:919-929.
14. Buonamici S, Li D, Chi Y, et al. EVI1 induces myelodysplastic syndrome in mice. J Clin Invest. 2004;114:713-719.
15. Lin YW, Slape C, Zhang Z, Aplan PD. NUP98-HOXD13 transgenic mice develop a highly penetrant, severe myelodysplastic syndrome that progresses to acute leukemia. Blood. 2005;106: 287-295.
16. Okuda T, van Deursen J, Hiebert SW, Grosveld G, Downing JR. AML1, the target of multiple chromosomal translocations in human leukemia, is essential for normal fetal liver hematopoiesis. Cell. 1996;84:321-330.
17. Wang Q, Stacy T, Binder M, et al. Disruption of the Cbfa2 gene causes necrosis and hematorrhaging in the central nervous system and blocks definitive hematopoiesis. Proc Natl Acad Sci U S A. 1996;93:3444-3449.
18. Ichikawa M, Asai T, Saito T, et al. AML-1 is required for megakaryocytic maturation and lymphocytic differentiation, but not for maintenance of hematopoietic stem cells in adult hematopoiesis. Nat Med. 2004;10:299-304.
19. Song WJ, Sullivan MG, Legare RD, et al. Haploinsufficiency of CBFA2 causes familial thrombocytopenia with propensity to develop acute myelogenous leukaemia. Nat Genet. 1999;23:166-175.
20. Michaud J, Wu F, Osato M, et al. In vitro analyses of known and novel RUNX1/AML1 mutations in dominant familial platelet disorder with predisposition to acute myelogenous leukemia: implications for mechanisms of pathogenesis. Blood. 2002;99:1364-1372.
21. Osato M, Asou N, Abdalla E, et al. Biallelic and heterozygous point mutations in the runt domain of the AML1/PEBP2alphaB gene associated with myeloblastic leukemias. Blood. 1999;93:1817-1824.
22. Preudhomme C, Warot-Loze D, Roumier C, et al. High incidence of biallelic point mutations in the Runt domain of the AML1/PEBP2alpha B gene in

Mo acute myeloid leukemia and in myeloid malignancies with acquired trisomy 21. Blood. 2000; 96:2862-2869.

23. Imai Y, Kurokawa M, Izutsu K, et al. Mutations of the AML1 gene in myelodysplastic syndrome and their functional implications in leukemogenesis. Blood. 2000;96:3154-3160.
24. Langabeer SE, Gale RE, Rollinson SJ, Morgan GJ, Linch DC. Mutations of the AML1 gene in acute myeloid leukemia of FAB types M0 and M7. Genes Chromosomes Cancer. 2002;34:24-32.
25. Harada H, Harada Y, Tanaka H, Kimura A, Inaba T. Implications of somatic mutations in the AML1 gene in radiation-associated and therapy-related myelodysplastic syndrome/acute myeloid leukemia. Blood. 2003;101:673-680.
26. Harada H, Harada Y, Niimi H, Kyo T, Kimura A, Inaba T. High incidence of somatic mutations in the AML1/RUNX1 gene in myelodysplastic syndrome and low blast percentage myeloid leukemia with myelodysplasia. Blood. 2004;103:2316-2324.
27. Osato M. Point mutations in the RUNX1/AML1 gene: another actor in RUNX leukemia. Oncogene. 2004;23:4284-4296.
28. Steensma DP, Gibbons RJ, Mesa RA, Tefferi A, Higgs DR. Somatic point mutations in RUNX1/CBFA2/AML1 are common in high-risk myelodysplastic syndrome, but not in myelofibrosis with myeloid metaplasia. Eur J Haematol. 2005;74:47-53.
29. Christiansen DH, Andersen MK, Pedersen-Bjergaard J. Mutations of AML1 are common in therapy-related myelodysplasia following therapy with alkylating agents and are significantly associated with deletion or loss of chromosome arm 7q and with subsequent leukemic transformation. Blood. 2004;104:1474-1481.
30. Yamashita N, Osato M, Huang L, et al. Haploinsufficiency of Runx1/AML1 promotes myeloid features and leukaemogenesis in BXH2 mice. Br J Haematol. 2005;131:495-507.
31. Morishita K, Parker DS, Mucenski ML, Jenkins NA, Copeland NG, Ihle JN. Retroviral activation of a novel gene encoding a zinc finger protein in IL-3-dependent myeloid leukemia cell lines. Cell. 1988;54:831-840.
32. Mucenski ML, Taylor BA, Ihle JN, et al. Identification of a common ecotropic viral integration site, Evi1, in the DNA of AKXD murine myeloid tumors. Mol Cell Biol. 1988;8:301-308.
33. Calmels B, Ferguson C, Laukkanen MO, et al. Recurrent retroviral vector integration at the Mds1/Evi1 locus in nonhuman primate hematopoietic cells. Blood. 2005;106:2530-2533.
34. Kustikova O, Fehse B, Modlich U, et al. Clonal dominance of hematopoietic stem cells triggered by retroviral gene marking. Science. 2005;308: 1171-1174.
35. Modlich U, Kustikkova OS, Schmidt M, et al. Leukemias following retroviral transfer of multidrug resistance 1 (MDR1) are driven by combinatorial insertional mutagenesis. Blood 2005;105:4235-4246.
36. Nucifora G, Laricchia-Robbio L, Senyuk V. Evi1 and hematopoietic disorders: history and perspectives. Gene. 2006;368:1-11.
37. Akagi K, Suzuki T, Stephens RM, Jenkins NA, Copeland NG. RTCGD: retroviral tagged cancer gene database. Nucleic Acids Res. 2004;32:523-527.
38. Jin G, Yamazaki Y, Takuwa M, et al. Trib1 and Evi1 cooperate with Hoxa and Meis1 in myeloid leukemogenesis. Blood. 2007;109:3998-4005.
39. Morita S, Kojima T, Kitamura T. Plat-E: an efficient and stable system for transient packaging of retroviruses. Gene Ther. 2000;7:1063-1066.
40. Kitamura T, Koshino Y, Shibata F, et al. 2003. Retrovirus-mediated gene transfer and expression cloning: powerful tools in functional genomics. Exp. Hematol. 2003;31:1007-1014.
41. Kogan SC, Ward JM, Anver MR, et al. Bethesda proposals for classification of nonlymphoid hematopoietic neoplasms in mice. Blood. 2002;100: 238-245.
42. Slape C, Hartung H, Lin YW, et al. Retroviral insertional mutagenesis identifies genes that collaborate with NUP98-HOXD13 during leukemic transformation. Cancer Res. 2007;67:5148-55.
43. Wimmer K, Vinatzer U, Zwirn P, et al. Comparative expression analysis of the antagonistic transcription factors EVI1 and MDS1-EVI1 in murine tissues and during in vitro hematopoietic differentiation. Biochem Biophys Res Commun. 1998; 252:691-6.
44. Riley J, Butler R, Ogilvie D, et al. A novel, rapid method for the isolation of terminal sequences from yeast artificial chromosome (YAC) clones. Nucl. Acids Res. 1990;18:2887-2890.
45. Arnold C, Hodgson IJ. Vectorette PCR: a novel approach to genome walking. PCR Methods Appl. 1991;1:39-42.
46. Tsuzuki S, Hong D, Gupta R, Matsuo K, Seto M, Enver T. Isoform-specific potentiation of stem and progenitor cell engraftment by AML1/RUNX1. PLoS Med. 2007;4:e172.
47. Riviere I, Brose K, Mulligan RC. Effects of retroviral vector design on expression of human adenosine deaminase in murine bone marrow transplant recipients engrafted with genetically modified cells. Proc Natl Acad Sci U S A. 1995; 92:6733-6737.
48. Langabeer SE, Rogers JR, Harrison G, et al. EVI1 expression in acute myeloid leukaemia. Br J Haematol. 2001;112:208-211.
49. Cuenco GM, Ren R. Both AML1 and EVI1 oncogenic components are required for the cooperation of AML1/MDS1/EVI1 with BCR/ABL in the induction of acute myelogenous leukemia in mice. Oncogene. 2004;23:569-579.
50. Louz D, van den Broek M, Verbakel S, et al. Erythroid defects and increased retrovirally-induced tumor formation in Evi1 transgenic mice. Leukemia. 2000;14:1876-1884.
51. Heuser M, Beutel G, Krauter J, et al. High meningioma 1 (MN1) expression as a predictor for poor outcome in acute myeloid leukemia with normal cytogenetics. Blood. 2006;108:3898-905.
52. Cuenco GM, Nucifora G, Ren R. Human AML1/MDS1/EVI1 fusion protein induces an acute myelogenous leukemia (AML) in mice: a model for human AML. Proc Natl Acad Sci USA. 2000;97: 1760-1765.

Peptidoglycan and lipopolysaccharide activate PLCγ2, leading to enhanced cytokine production in macrophages and dendritic cells

Daisuke Aki[1,2], Yasumasa Minoda[1], Hideyuki Yoshida[1], Satoko Watanabe[1], Ryoko Yoshida[1], Giichi Takaesu[1], Takatoshi Chinen[1], Toshiya Inaba[2], Masaki Hikida[3], Tomohiro Kurosaki[3], Kazuko Saeki[1] and Akihiko Yoshimura[1,*]

[1]*Division of Molecular and Cellular Immunology, Medical Institute of Bioregulation, Kyushu University, Maidashi, Higashi-ku, Fukuoka 812-8582, Japan*

[2]*Department of Molecular Oncology and Leukemia Program Project, Research Institute for Radiation Biology and Medicine, Hiroshima University, Kasumi, Minami-ku, Hiroshima 734-8553, Japan*

[3]*Laboratory for Lymphocyte Differentiation, RIKEN Research Center for Allergy and Immunology, 1-7-22, Suehirocho, Tsurumi-ku, Yokohama, Kanagawa 230-0045, Japan*

In macrophages and monocytes, microbial components trigger the production of pro-inflammatory cytokine through Toll-like receptors (TLRs). Although major TLR signaling pathways are mediated by serine/threonine kinases, including TAK1, IKK and MAP kinases, tyrosine phosphorylation of intracellular proteins by TLR ligands has been suggested in a number of reports. Here, we demonstrated that peptidoglycan (PGN) of a Gram-positive bacterial cell wall component, a TLR2 ligand and lipopoysaccharide (LPS) of a Gram-positive bacterial component, a TLR4 ligand induced tyrosine phosphorylation of phospholipase Cγ-2 (PLCγ2), leading to intracellular free Ca^{2+} mobilization in bone marrow-derived macrophages (BMMϕ) and bone marrow-derived dendritic cells (BMDC). PGN- and LPS-induced Ca^{2+} mobilization was not observed in BMDC from PLCγ2 knockout mice. Thus, PLCγ2 is essential for TLR2 and TLR4-mediated Ca^{2+} flux. In PLCγ2-knockdown cells, PGN-induced IκB-α phosphorylation and p38 activation were reduced. Moreover, PLCγ2 was necessary for the full production of TNF-α and IL-6. These data indicate that the PLCγ2 pathway plays an important role in bacterial ligands-induced activation of macrophages and dendritic cells.

Introduction

Toll-like receptors (TLRs), which recognize the structure of microorganisms, are essential for innate immune signaling (Akira 2003; Akira *et al.* 2006). Peptidoglycan (PGN) is a major component of the cell wall of Gram-positive bacteria, and it activates the innate immune system of the host. TLR2 has been shown to be a main receptor recognizing PGN, and its activation in response to PGN induces the production of pro-inflammatory cytokines, chemokines and adhesion molecules (Akira *et al.* 2006; O'Neill & Bowie 2007). For TLR2 signaling, TLR2 utilizes adaptor proteins Myeloid differentiation 88 (MyD88) and MyD88-adaptor like (Mal) to activate IL-1 receptor-associated kinase. Then, the activated IL-1 receptor-associated kinase dissociates the MyD88/Mal complex from the receptor, followed by association with tumor necrosis factor-associated factor 6 (TRAF6). This triggers the activation of the Rel family transcription factor NF-κB, which is required for transactivation of gene expression (Akira *et al.* 2006; O'Neill *et al.* 2007). In addition, MAP kinases, including p38, JNK and ERK, are also activated in response to PGN, which leads to activation of AP-1 and ATF2 transcription factors (Chang *et al.* 2005).

In lymphocytes, Ca^{2+} is important for cellular function as a second messenger (Gallo *et al.* 2006). It is generally established that ligation of antigen receptors induces the generation of inositol-1,4,5-triphospate (IP_3) and

Communicated by: Tetsuya Taga
**Correspondence*: E-mail: yakihiko@bioreg.kyushu-u.ac.jp

DOI: 10.1111/j.1365-2443.2007.01159.x

diacylglycerol (DAG). IP_3 binds to IP_3R in the membrane of the endoplasmic reticulum (ER) and induces the release of Ca^{2+} into the cytoplasm, whereas DAG, together with Ca^{2+}, activates protein kinase C (PKC) (Berridge 1993; Nishizuka 1995; Carpenter & Ji 1999). Recent studies suggest that the Ca^{2+} flux is also activated via TLR signaling (Chun & Prince 2006; Zhou *et al.* 2006). The TLR2 ligand, Pam_3Cys-Ser-Lys_4 (P3C), stimulated the release of Ca^{2+} by activating TLR2 phosphorylation by c-Src and recruited phosphatidylinositol 3-kinase (PI3K) and phospholipase Cγ (PLCγ) to affect Ca^{2+} release through IP_3 in airway epithelial cells (Chun & Prince 2006). Furthermore, Ca^{2+} release has also been shown to increase upon the stimulation of TLR4 (Zhou *et al.* 2006). However, few studies have demonstrated a direct contribution of PLCγ2 to the PGN-induced Ca^{2+} mobilization. Furthermore, the importance of this pathway for pro-inflammatory cytokine production has not been elucidated.

In this study, we investigated a loss-of-function effect of PLCγ2 in PGN-stimulated macrophages and dendritic cells. PLCγ2 depletion using siRNA reduced PGN-induced p38, Akt and IκB-α phosphorylation in murine macrophage RAW 264.7 cells. Moreover, PGN and lipopolysaccharide (LPS) stimulation failed to activate TLR2- and TLR4-dependent Ca^{2+} mobilization in bone marrow-derived dendritic cells (BMDC) from Tie2Cre/PLCγ2$^{flox/flox}$ mutant mice. PLCγ2 knockdown in RAW264.7 cells and knockout in bone marrow-derived macrophages (BMMϕ) resulted in a reduction in the production of TNF-α, IL-6 in response to PGN. Our results indicated that Ca^{2+} mobilization plays an important role in pro-inflammatory cytokine production induced by the PGN/TLR2 as well as the LPS/TLR4 pathways.

Results

PGN-and LPS-induced tyrosine phosphorylation of PLCγ2 in BMMϕ and BMDC

Previously, we identified several tyrosine-phosphorylated proteins in LPS-activated RAW 264.7 cells using proteomic approaches. Among them, we noticed PLCγ2 (Aki *et al.* 2005). To confirm the tyrosine phosphorylation of PLCγ2 in the stimulation to LPS, we performed immunoblot analysis using an anti-phosphotyrosine (4G10) and PLCγ2 antibody in LPS-stimulated BMDC. As a result, the tyrosine phosphorylation level of PLCγ2 was increased after 30 min of LPS stimulation (Fig. 1A). Furthermore, we found that PGN, one of the bacterial ligands for TLR2, also induced tyrosine phosphorylation of PLCγ2. As shown in Fig. 1B, total cell lysates from RAW264.7 cells were isolated 0, 15, 30, 60 and 180 min after stimulation with PGN. Tyrosine-phosphorylated proteins were immunoprecipitated with 4G10 and immunoblotted with anti-PLCγ2 antibody or 4G10. Tyrosine phosphorylation of PLCγ2 increased within 30 min of PGN stimulation (Fig. 1B). To investigate whether tyrosine phosphorylation of PLCγ2 is induced in response to other TLR ligands, we examined the effects of zymosan (TLR2), Poly(I:C) (TLR3) and CpG-ODN (TLR9). As a result, tyrosine-phosphorylation of PLCγ2 was induced by zymosan as well as LPS and PGN, but Poly(I:C) and CpG-ODN which is mimic a viral infection failed to induce ligands-dependent PLCγ2 tyrosine-phosphorylation (Fig. 1C). This data indicated that PLCγ2 is induced tyrosine-phosphorylation by TLR2 and TLR4 stimulation. In addition, after pre-treatment with the tyrosine kinases inhibitor PP2 in BMMϕ, PGN-induced PLCγ2 tyrosine phosphorylation was completely inhibited (Fig. 1D), suggesting that tyrosine phosphorylation of PLCγ2 is PTKs-dependent. Interestingly, PLCγ2 tyrosine phosphorylation continued for 180 min (Fig. 1B). This suggests an indirect effect of PGN on the tyrosine phosphorylation of PLCγ2. Thus, BMMϕ were pre-treated with a translational inhibitor, cycloheximide for 30 min and then treated with PGN for 180 min. PGN-induced tyrosine phosphorylation of PLCγ2, as well as the tyrosine phosphorylation of the entire protein, was partially inhibited by cycloheximide (Fig. 1E). These data suggest that PLCγ2 was tyrosine-phosphorylated by direct activation of tyrosine kinases and an indirect effect, which required a new protein synthesis.

PGN induces intracellular Ca^{2+} mobilization in macrophages and dendritic cells

To examine whether TLR-ligands can induce intracellular Ca^{2+} mobilization, BMMϕ were loaded with Fluo-3/AM and then stimulated with PGN and their fluorescence intensity was measured using confocal microscope. A transient increase in fluorescence intensity was induced after PGN treatment (Fig. 2A). The concentration of Ca^{2+} reached its maximum level within a few seconds and quickly returned to the baseline level (Fig. 2A). In BMDC, similar PGN-dependent intracellular Ca^{2+} mobilization to that for BMMϕ was induced (Fig. 2B). Moreover, we also observed that LPS stimulation also induced Ca^{2+} mobilization in BMDC (Fig. 2C). These results indicated that bacterial ligands caused a transient increase in the concentration of Ca^{2+} via TLR signaling in BMMϕ and BMDC.

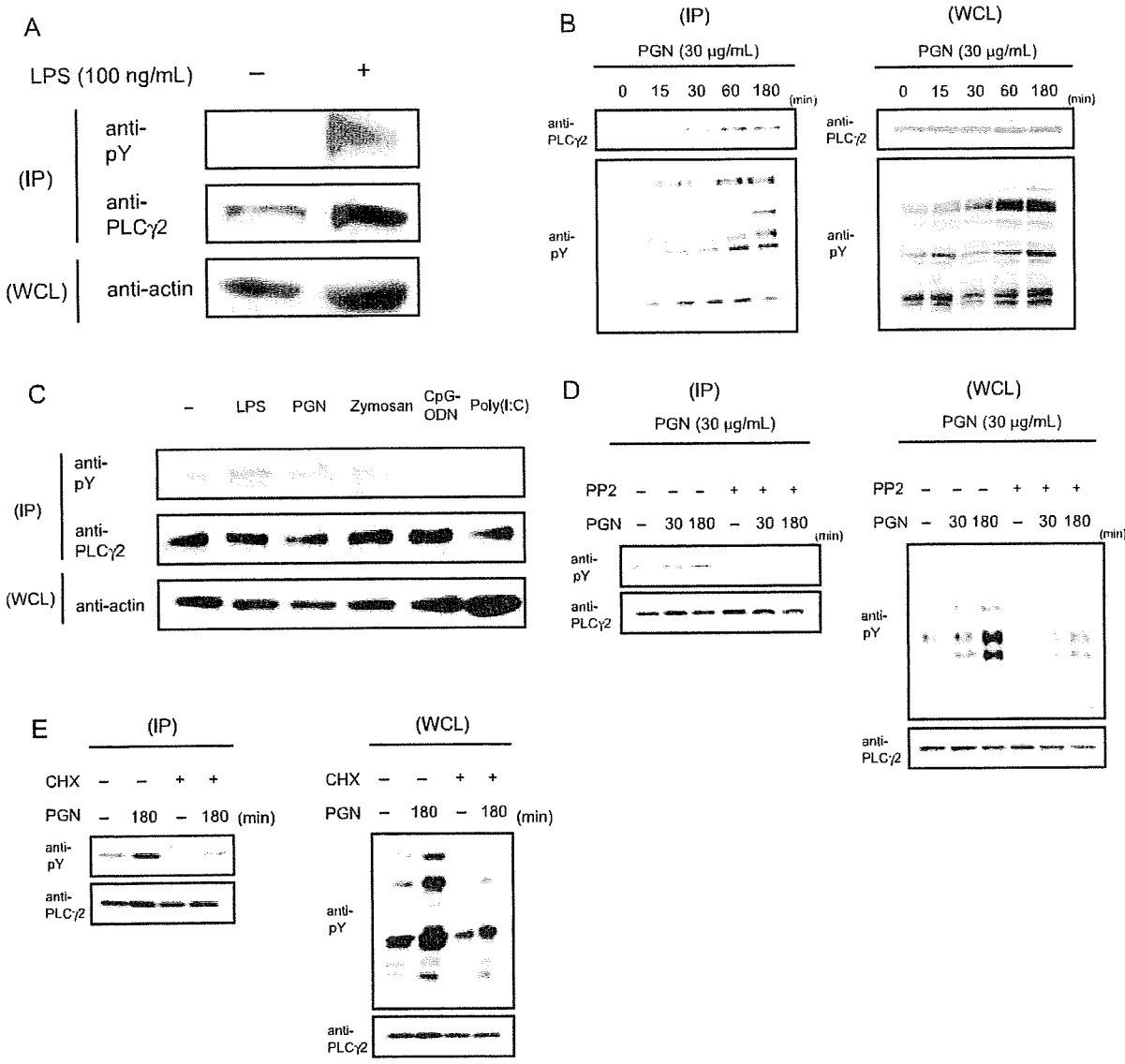

Figure 1 TLR2 and TLR4 signaling induced tyrosine phosphorylation of PLCγ2. (A) BMDC were stimulated with 100 ng/mL LPS for 30 min. Cell extracts were immunoprecipitated with anti-PLCγ2 antibody and then immunoblotted with anti-phosphotyrosine antibody (4G10). (B) RAW264.7 cells were stimulated with 30 μg/mL PGN for the indicated time and then lysed. Cell extracts were immunoprecipitated with 4G10 and then immunoblotted with anti-PLCγ2 antibody. (C) BMMϕ were stimulated with 1 μg/mL LPS, 20 μg/mL PGN, 20 μg/mL zymosan, 1 μM CpG-ODN or 100 μg/mL Poly(I : C) for 180 min. Cell extracts were immunoprecipitated with anti-PLCγ2 antibody and then immunobloted with the indicated antibodies. (D, E) BMMϕ were pre-treated with 10 μM PP2 for 15 min (D) and 10 μM cycloheximide for 30 min (E) and then stimulated with PGN for the indicated period. Cell extracts were immunoprecipitated with anti-PLCγ2 antibody and immunoblotted with 4G10.

PLCγ2 is required for PGN- and LPS-induced Ca^{2+} signaling

The Ca^{2+} flux is essential for many cellular responses. Inositol 1,4,5-triphosphate (IP_3) generated by PLCγ has been shown to be responsible for Ca^{2+} mobilization from the ER (Berridge 1993; Nishizuka 1995; Carpenter & Ji 1999). To elucidate whether PLCγ2 is involved in Ca^{2+} mobilization in response to PGN, we first assessed the effect of a PLC inhibitor, U73122, on PGN-stimulated hTLR2-expressing HEK 293 cells. U73122 pre-treatment for 30 min, but not DMSO, blocked PGN-induced

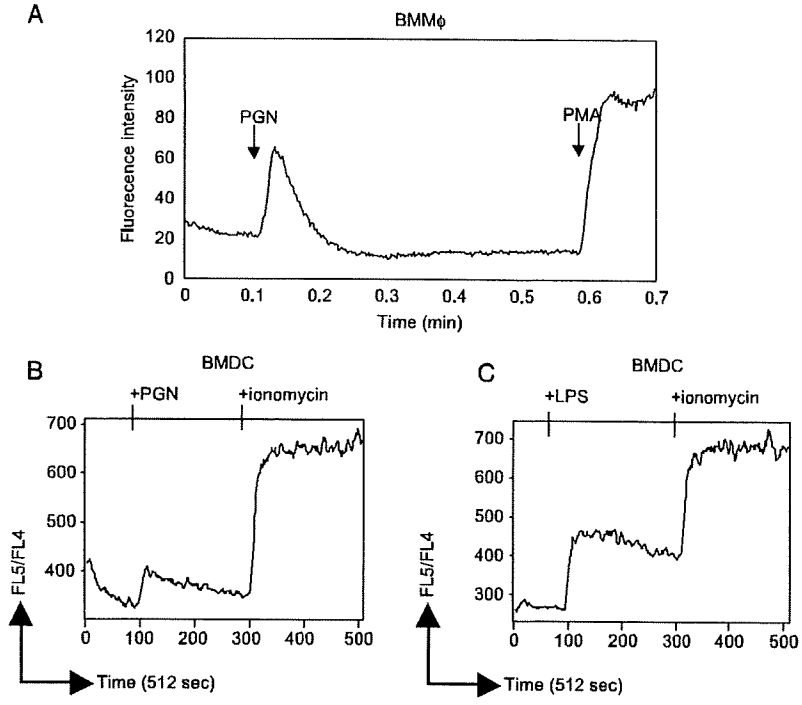

Figure 2 TLR2 and TLR4 activate intracellular Ca^{2+} mobilization in BMMϕ and BMDC. (A) BMMϕ were loaded with Fluo-3/AM and stimulated with 50 μg/mL PGN. (B, C) BMDC were loaded onto Indo-1 AM and then stimulated with 50 μg/mL PGN (B) or 100 ng/mL LPS (C). Intracellular Ca^{2+} mobilization was evaluated as described in Experimental procedures. Sequentially, these cells were stimulated with PMA or ionomycin as positive controls. The data shown are representative of several experiments that produced similar results.

intracellular Ca^{2+} mobilization (Fig. 3A). Next, to confirm the essential role of PLCγ2 in TLR-mediated intracellular Ca^{2+} mobilization, we generated Tie2-Cre PLCγ2$^{flox/flox}$ mice. PLCγ2$^{flox/flox}$ mice, in which an exon encoding the phosphatidylinositol-4, 5-biphosphate (PIP_2) binding site of the PLCγ2 gene is flanked by two loxP sites, have been described elsewhere (Hashimoto *et al.* 2000). The PLCγ2 gene was efficiently deleted in BMDC from homozygous mutant mice (Fig. 3B). We then examined the PGN-induced intracellular Ca^{2+} release of BMDC from Tie2-Cre PLCγ2$^{flox/flox}$ mice. PGN-mediated Ca^{2+} mobilization was completely blocked in the BMDC from mutant mice (Fig. 3C). This result was consistent with a blocking effect of U73122 on Ca^{2+} mobilization in PGN-treated HEK293 cells stably expressing TLR2 (Fig. 3A). In addition, the LPS-induced transient Ca^{2+} increase was also significantly inhibited in BMDC from Tie2-Cre PLCγ2$^{flox/flox}$ mutant mice (Fig. 3D). These data indicate that PLCγ2 is necessary for intracellular Ca^{2+} mobilization in response to TLR stimulation in BMMϕ and BMDC.

TLR2-PLCγ2 signaling pathway is involved in PGN-induced p38, Akt, IκB-α and pro-inflammatory cytokine production

To explore the physiological role of PLCγ2 in TLR signaling, we generated RAW264.7 cells that were transfected with a vector expressing PLCγ2 siRNA. Immunoblot analysis indicated the silencing of PLCγ2 expression in RAW264.7 cells by PLCγ2 siRNA. The reduction of PLCγ2 levels by siRNA was greater in #2 than in #1 (Fig. 4A).

NF-κB, MAPK and Akt pathways are known to be the major downstream pathways in TLR signaling (Arbibe *et al.* 2000; Akira *et al.* 2006). As shown in Fig. 4B, silencing of PLCγ2 diminished the PGN-induced phosphorylation of p38, Akt and IκB-α. However, ERK phosphorylation was indistinguishable from empty vector-transfected cells (Fig. 4B). We next analyzed PGN-induced pro-inflammatory cytokines in PLCγ2 knockdown cells. PGN-induced IL-6 production from PLCγ2 knockdown cells #2 was strongly reduced. This reduction in knockdown cells #2 was due to the suppression of mRNA synthesis. Little difference was observed in PLCγ2 knockdown cells #1, where PLCγ2 level was not greatly different from that in empty vector transfected cells. TNF-α secretion was slightly inhibited in PLCγ2 knockdown cells #2; on the other hand, it was normal in knockdown cells #1 (Fig. 4C).

Finally, we found that, upon stimulation of PLCγ2$^{flox/flox}$ BMMϕ with PGN, IL-6 and TNF-α production were suppressed to 50% and 37% of the control levels, respectively (Fig. 4D). Furthermore, LPS stimulation of PLCγ2$^{flox/flox}$ BMMϕ inhibited cytokine production to

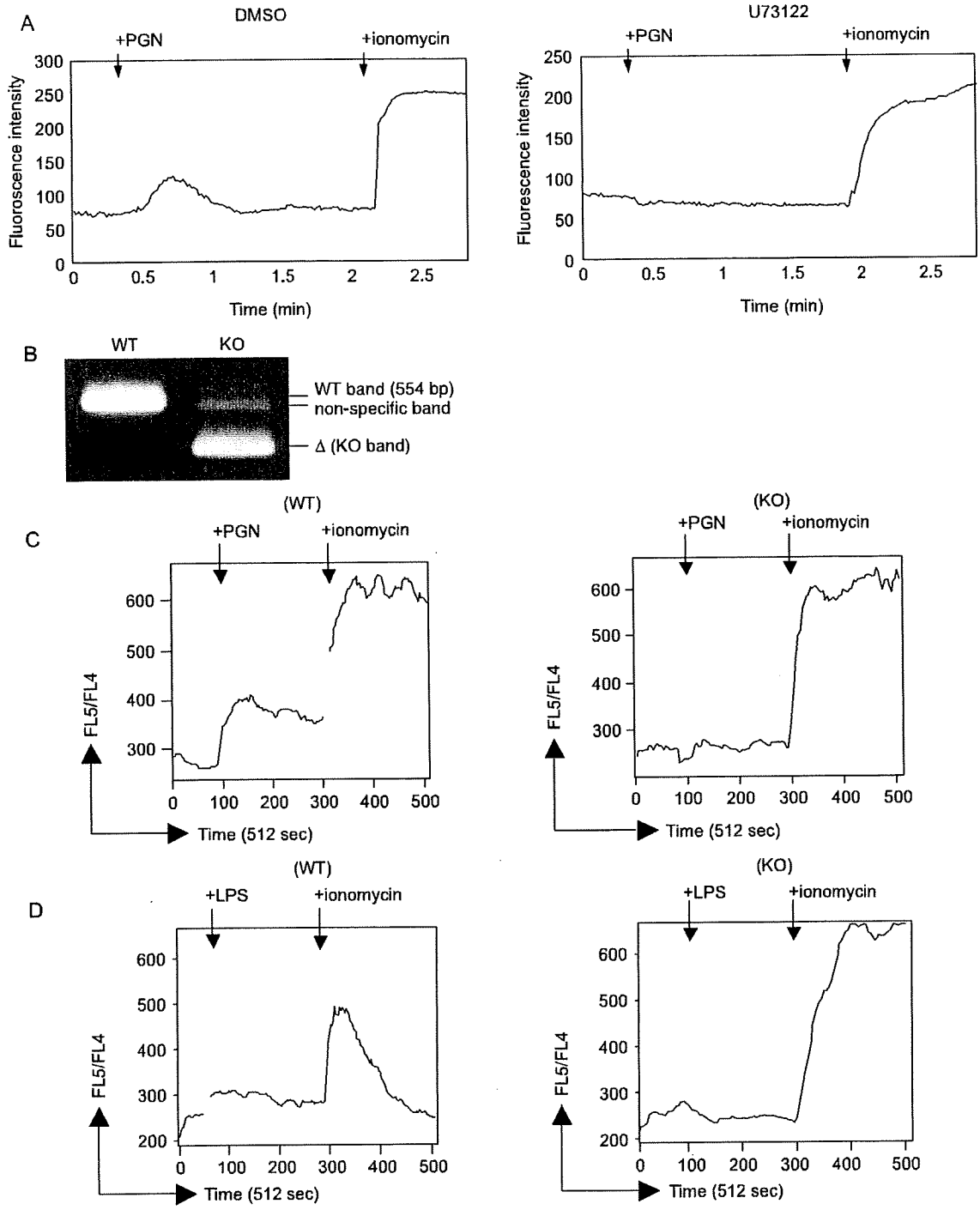

Figure 3 PLCγ2 is essential for TLR-dependent Ca^{2+} signaling. (A) HEK293 stably expressing hTLR2 cell lines were stimulated with 50 μg/mL PGN after pre-treatment with DMSO or 10 μM U73122. Cells were imaged using confocal microscope. (B) PCR analysis of genomic DNA from BMDC. The PCR product of wild-type PLCγ2 locus is 554 bp. In Tie2-Cre $PLC\gamma2^{fl/fl}$ mice, a band of 386 bp, Δ (KO band), indicates the Cre-mediated deletion of PLCγ2. (C, D) BMDC from wild-type and mutant mice stimulated with 30 μg/mL PGN (C) or 100 ng/mL LPS (D) were analyzed by flow cytometric analysis as described in Experimental procedures.

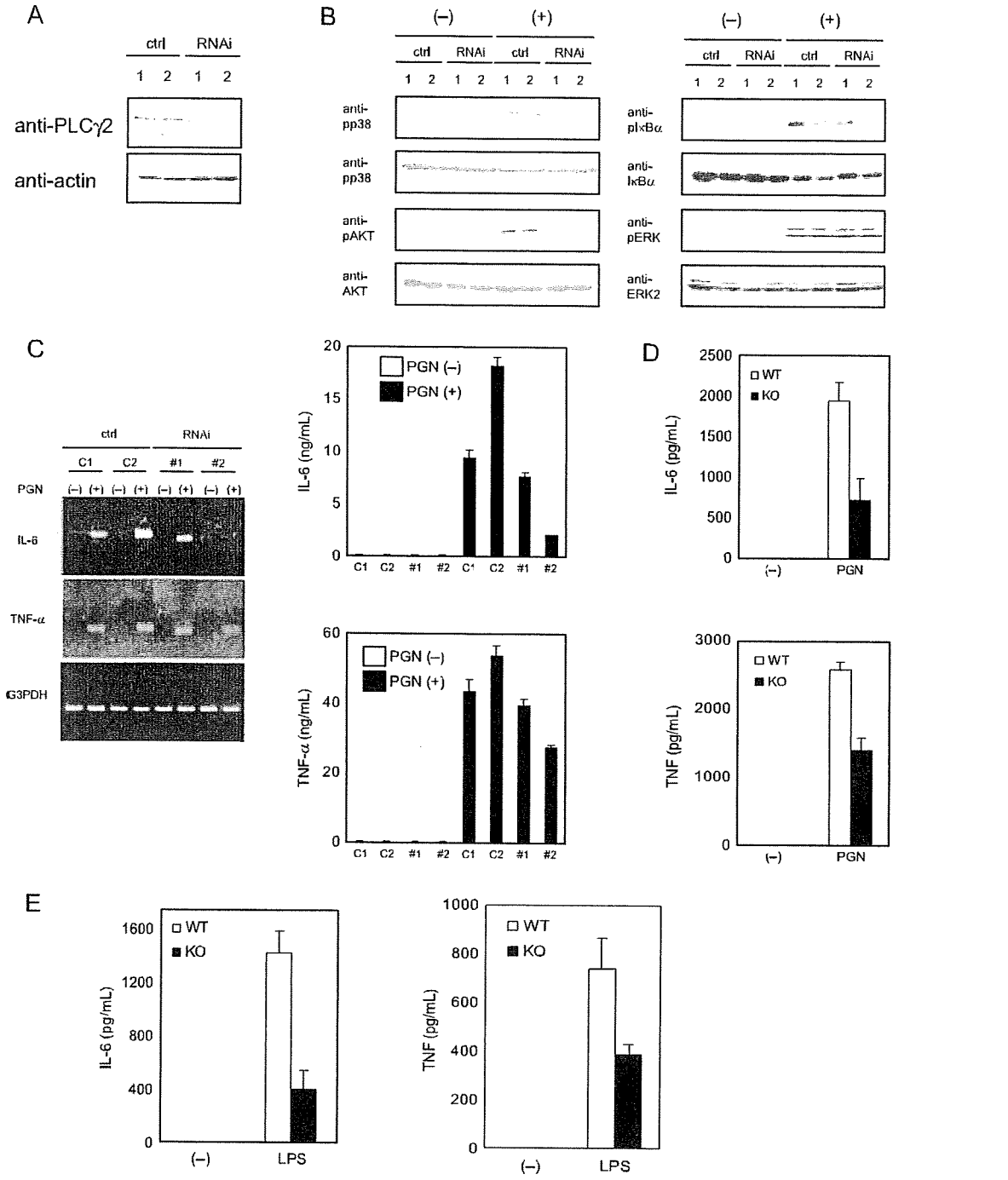

Figure 4 PLCγ2 regulates TLR signaling and pro-inflammatory cytokine production. Two individual RAW 264.7 transformants, each containing vector alone as control or PLCγ2 siRNA expression construct, were analyzed. (A) cell extracts were immunoblotted with the indicated antibodies. (B) Transformants were stimulated with 30 μg/mL PGN. The levels of IκB-α and phospho-IκB-α were determined 15 min after stimulation. Those of p38, Akt and Erk were measured 30 min after stimulation. (C–E) For RT-PCR analysis, cells were stimulated with PGN for 1 h and then total RNA was extracted from the cells (C). For ELISA, cells were stimulated with 30 μg/mL PGN (C, D) or 100 ng/mL LPS (E) for 6 h, and IL-6 and TNF-α in the cell culture supernatants were then analyzed.

the same degree as PGN stimulation did (Fig. 4E). These data suggest that PLCγ2 is required for pro-inflammatory cytokine production mediated by PGN-and LPS-dependent Ca^{2+} flux in BMMϕ and BMDC.

Discussion

In agreement with our present study, several recent studies have demonstrated that TLRs induced rapid changes in the intracellular Ca^{2+} concentration (Supajatura *et al.* 2002; Kim *et al.* 2004; Chun & Prince 2006; Zhou *et al.* 2006). Ca^{2+} signaling regulates downstream signaling molecules, such as nuclear factor of activated T cells transcriptional complexes (NF-ATc) and calcineurin, followed by many cellular responses through the change of gene expression (Gallo *et al.* 2006). It has been shown that Ca^{2+}-dependent signaling pathway results in the gene expression of inducible nitric-oxide synthase as well as the production of TNF-α upon LPS stimulation of rat peritoneal macrophages (Zhou *et al.* 2006). Furthermore, it has been suggested that TLR-dependent PLCγ2 activation participated in this event (Shinji *et al.* 1997; Chun & Prince 2006; Zhou *et al.* 2006). However, there has been little direct evidence for the involvement of PLCγ2 in Ca^{2+} mobilization in response to TLR ligands. In the present study, we found that PGN and LPS stimulation induced PLCγ2 phosphorylation and intracellular Ca^{2+} mobilization in BMMϕ and BMDC. We clearly demonstrated that this pathway played an important role in the activation of macrophages using PLCγ2 knockdown cells and BMMϕ from PLCγ2-disrupted mice. Thus, it is now clear that PLCγ2 plays an important role in TLR2 and TLR4-mediated Ca^{2+} mobilization and signal transduction.

There are several important questions still to be solved. First, the manner in which TLR2 and TLR4 signaling is activated is not exactly clear. TLR2-dependent PLCγ2 tyrosine phosphorylation was clearly detected at 30 min after PGN stimulation, and tyrosine phosphorylation seemed to be amplified at 180 min. Tyrosine phosphorylation of PLCγ2 at this point was not fully inhibited by cycloheximide pre-treatment; thus, there seem to be both direct and indirect pathways for PLCγ2 tyrosine phosphorylation by PGN stimulation. When PP2 was used, the phosphorylation of PLCγ2 induced by PGN was completely inhibited. This result suggested that Src family tyrosine kinases are directly involved in TLR2 signaling, as previously reported (Chun & Prince 2006). Other tyrosine kinases were required for the activation of TLR2 signaling. In particular, Syk kinase was considered to be involved in TLR2 signaling. Syk-deficient dendritic cells were unable to produce IL-2 and IL-10. In addition, Syk binds to the phosphorylation YxxL motif of the β-glucan receptor, Dectin-1, upon ligand binding. It is, therefore, suggested that Syk is recruited to the Dectin-1 phosphorylation site and participates in TLR2 signaling events (Rogers *et al.* 2005). Moreover, recent studies have demonstrated that a member of Tec family tyrosine kinase, Btk has important implications for TLR signal transduction. It has been demonstrated that Btk tyrosine phosphorylation was TLR2-dependent and the lack of Btk resulted in lower amounts of TNF-α and IL-1β production (Jefferies *et al.* 2003; Horwood *et al.* 2006). However, the question of how these tyrosine kinases are activated by PGN is unanswered. In addition, the question of how these kinases phosphorylate PLCγ2 is still not very clear.

Second, an important question is how downstream PLCγ2 is involved in TLR signaling. Apparently, the activation of PLCγ2 results in an increase of intracellular Ca^{2+} and DAG. Ca^{2+} activates NF-AT transcription factors, while DAG activates PKC. PKCα/β has been shown to participate in NF-κB activation upon LPS stimulation of macrophages (Asehnoune *et al.* 2005; Zhou *et al.* 2006). Cyclosporine, an inhibitor of Ca^{2+}-dependent NF-AT activation, has been shown to block cytokine production (Duperrier *et al.* 2002; Chen *et al.* 2004). Thus, both the Ca^{2+}-NFAT and the DAG-PKC pathways seem to be important for the downstream of PLCγ2 activated by TLRs. However, the precise role of NF-AT and PKC in cytokine production remains to be clarified. Furthermore, it has been shown that another PKC isoform, PKCε, is also involved in LPS signaling (Shapira *et al.* 1997; Valledor *et al.* 2000; Castrillo *et al.* 2001; McGettrick *et al.* 2006). However, it has not been clarified which PKCs isoform was activated by TLR2-PLCγ2 pathway.

The knockdown of PLCγ2 is effective enough to inhibit Akt activation in particular. The pathway for Akt activation in response to TLR ligands has not been clarified. We found that Akt activation was reduced in not only PLCγ2-knockdown cells, but also U73122 treated RAW264.7 cells (data not shown). Thus, our data raise an interesting possibility that PLCγ2 is an upstream of PI3kinase-Akt. On the other side, the generation of PIP_3 by PI3K also activates PLCγ2 (Bae *et al.* 1998). A recent study demonstrated that phosphorylated PLCγ1 interacted with Akt in response to EGF stimulation (Wang *et al.* 2006). Thus, Akt could be a downstream target of PLCγ2. We have shown that the suppression of PLCγ2 resulted in the reduction of IκB-α, p38 phosphorylation as well as Akt. The mechanism underlying these suppressions has not been clarified. It has been demonstrated that the PKC-CARD pathway is critical for NF-κB activation in response to T cell receptor ligation (Hara

et al. 2004). Several reports indicate that PKC is important for TLR signaling and cytokine production in macrophages (Chen *et al.* 1998; Castrillo *et al.* 2001; Zhou *et al.* 2006). However, the contribution of this pathway has not been clarified because NF-κB is strongly activated by the TRAF6-TAK1-IKK pathways. Furthermore, it is not known which pathway, Ca^{2+} or PKC, directly regulates p38 or Akt. Further study is necessary to define the link between PLCγ2 and these pathways.

Experimental procedures

Antibodies and reagent

Peptidoglycan (PGN) from *Staphylococcus aureus* was purchased from Fluka (Bachs, Sweden). PP2, cyclohexamide and wortmannin were from Calbiochem (San Diego, CA). LPS, CpG-ODN and Poly(I : C) were from Sigma-Aldrich (Seelze, Germany). Zymosan was obtained from Invitrogen (Carlsbad, CA). Antibodies against PLCγ2 (Q-20), IκB-α (C-21) and ERK2 (C-14) were from Santa Cruz Biotechnology (Santa Cruz, CA). The anti-actin rabbit polyclonal antibody was purchased from Sigma (St. Louis, MO). Antibodies against Akt, p38, phospho-IκBα, phospho-p40/p42 MAP kinase, phospho-p38, phospho-Akt and 4G10 have been described (Aki *et al.* 2005).

Mice

$PLC\gamma2^{flox/flox}$ mice and Tie2-cre transgenic mice have been previously established (Hashimoto *et al.* 2000; Kimura *et al.* 2004; Matsumura *et al.* 2007). Tie2-cre transgenic mice were bred with $PLC\gamma2^{flox/flox}$ mice to generate mice in which PLCγ2 was deleted in hemopoietic cells. All experiments were approved by the Animal Ethics Committee of Kyushu University.

Cell culture

TLR2 stably expressing HEK293 cells were prepared by transfection of hTLR2 cDNA and selected in the presence of G418. TLR2-HEK293 cells and the murine macrophage cell line RAW264.7 cells were cultured in DMEM supplemented with 10% fetal calf serum. To prepare BMMϕ, bone marrow cells were obtained from femora and tibia of 6–8-week-old C57BL6/J mice and then cultured in RPMI 1640 medium supplemented with 10% fetal bovine serum; the culture medium was conditioned by the L929 cells containing a macrophage colony-stimulating factor (M-CSF). After 7 days, the cells were used as BMMϕ for the experiments. BMDC were prepared as described elsewhere (Matsumura *et al.* 2007).

Immunoprecipitation and immunoblotting analysis

After stimulation, cells were washed with PBS and solubilized for 30 min at 4 °C in lysis buffer (Aki *et al.* 2005). Cell extracts were then centrifuged, and supernatants were used for immunoprecipitation with specific antibodies. After separation by SDS-PAGE and transfer to polyvinyliden difluoride membranes, proteins were analyzed by immunoblotting with the indicated antibodies.

Measurement of cytokine

The cells were plated on 6-well plates on the day before PGN stimulation. For ELISA, the cells were stimulated with PGN for 6 h. Then, culture supernatants were collected and analyzed for TNF-α and IL-6 (BD Biosciences PharMingen, San Diego, CA). For the analysis of mRNA expression, the cells were stimulated with PGN for 1 h. TNF-α and IL-6 RT-PCR were carried out as described (Aki *et al.* 2005; Chinen *et al.* 2006).

RNA interference

The small interfering RNA sequence that targets mouse PLCγ2 was at positions 1017–1037 (5′-GTCCTCCACGGAAGCGTATAT-3′). The annealed oligonucleotides were inserted into psiRNA-hH1neo expression vector (InvivoGen, San Diego, CA). Stable transformants were selected in 1 mg/mL G418.

Ca^{2+} flux analysis

For imaging, cells were grown in coverglass chamberslides and loaded for 30 min at 37 °C with 5 μM Fluo3/AM (DOJINDO) in the dark. Cells were washed with HANKS buffer. Fluorescence imaging was obtained using Carl Zeiss LSM 510 META scanning confocal microscope and analyzed using LSM Image Browse. For flow cytometric analysis, 1.0×10^7 BMDC cells were suspended in 10 mL of RPMI medium supplemented and loaded with 3 μM Indo-1 AM (Molecular Probes, Eugene, OR) at 37 °C for 30 min. After washing, 1.0×10^6 cells were used for analysis. The filter set-up on the BD LSR for Indo-1 was FL-5 424/444 nm BF filter and unbound Indo-1 FL-4 530/530 nm BF filter. The Ca^{2+} flux was measured as the ratio between the calcium bound Indo-1 and unbound or FL-5/FL-4 vs. time. Full-scale deflection of the Ca^{2+} flux was measured by the addition of 3.0 μg/mL ionomycin.

Acknowledgements

We thank Dr T. Muta (University of Tohoku) for hTLR2 cDNAs, Ms T. Yoshioka and M. Ohtsu for technical assistance, and Ms Y. Nishi for manuscript preparation. This study was supported by special Grants-in-Aid from the Ministry of Education, Culture, Sports, Science, and Technology of Japan, the Program for Promotion of Fundamental Studies in Health Sciences of the National Institute of Biomedical Innovation (NIBIO), the Naito Memorial Foundation, the Takeda Science Foundation, the Mochida Memorial Foundation, the Kato Memorial Foundation, the Kanae Foundation for the promotion of Medical Science, Clinical Research Foundation, the Osaka Cancer research Foundation, Mitsubishi Pharma Research Foundation and the Ichiro Kanehara Memorial Foundation.

References

Aki, D., Mashima, R., Saeki, K., Minoda, Y., Yamauchi, M. & Yoshimura, A. (2005) Modulation of TLR signalling by the C-terminal Src kinase (Csk) in macrophages. *Genes Cells* **10**, 357–368.

Akira, S. (2003) Toll-like receptor signaling. *J. Biol. Chem.* **278**, 38105–38108.

Akira, S., Uematsu, S. & Takeuchi, O. (2006) Pathogen recognition and innate immunity. *Cell* **124**, 783–801.

Arbibe, L., Mira, J.P., Teusch, N., Kline, L., Guha, M., Mackman, N., Godowski, P.J., Ulevitch, R.J. & Knaus, U.G. (2000) Toll-like receptor 2-mediated NF-κB activation requires a Rac1-dependent pathway. *Nat. Immunol.* **1**, 533–540.

Asehnoune, K., Strassheim, D., Mitra, S., Yeol Kim, J. & Abraham, E. (2005) Involvement of PKCα/β in TLR4 and TLR2 dependent activation of NF-κB. *Cell. Signal.* **17**, 385–394.

Bae, Y.S., Cantley, L.G., Chen, C.S., Kim, S.R., Kwon, K.S. & Rhee, S.G. (1998) Activation of phospholipase C-γ by phosphatidylinositol 3,4,5-trisphosphate. *J. Biol. Chem.* **273**, 4465–4469.

Berridge, M.J. (1993) Inositol trisphosphate and calcium signalling. *Nature* **361**, 315–325.

Carpenter, G. & Ji, Q. (1999) Phospholipase C-γ as a signal-transducing element. *Exp. Cell Res.* **253**, 15–24.

Castrillo, A., Pennington, D.J., Otto, F., Parker, P.J., Owen, M.J. & Bosca, L. (2001) Protein kinase Cepsilon is required for macrophage activation and defense against bacterial infection. *J. Exp. Med.* **194**, 1231–1242.

Chang, Y.J., Wu, M.S., Lin, J.T. & Chen, C.C. (2005) Helicobacter pylori-Induced invasion and angiogenesis of gastric cells is mediated by cyclooxygenase-2 induction through TLR2/TLR9 and promoter regulation. *J. Immunol.* **175**, 8242–8252.

Chen, C.C., Wang, J.K. & Lin, S.B. (1998) Antisense oligonucleotides targeting protein kinase C-α,-βI, or -δ but not -η inhibit lipopolysaccharide-induced nitric oxide synthase expression in RAW 264.7 macrophages: involvement of a nuclear factor κB-dependent mechanism. *J. Immunol.* **161**, 6206–6214.

Chen, T., Guo, J., Yang, M., Han, C., Zhang, M., Chen, W., Liu, Q., Wang, J. & Cao, X. (2004) Cyclosporin A impairs dendritic cell migration by regulating chemokine receptor expression and inhibiting cyclooxygenase-2 expression. *Blood* **103**, 413–421.

Chinen, T., Kobayashi, T., Ogata, H., Takaesu, G., Takaki, H., Hashimoto, M., Yagita, H., Nawata, H. & Yoshimura, A. (2006) Suppressor of cytokine signaling-1 regulates inflammatory bowel disease in which both IFNγ and IL-4 are involved. *Gastroenterology* **130**, 373–388.

Chun, J. & Prince, A. (2006) Activation of Ca^{2+}-dependent signaling by TLR2. *J. Immunol.* **177**, 1330–1337.

Duperrier, K., Farre, A., Bienvenu, J., Bleyzac, N., Bernaud, J., Gebuhrer, L., Rigal, D. & Eljaafari, A. (2002) Cyclosporin A inhibits dendritic cell maturation promoted by TNF-α or LPS but not by double-stranded RNA or CD40L. *J. Leukoc. Biol.* **72**, 953–961.

Gallo, E.M., Cante-Barrett, K. & Crabtree, G.R. (2006) Lymphocyte calcium signaling from membrane to nucleus. *Nat. Immunol.* **7**, 25–32.

Hara, H., Bakal, C., Wada, T., Bouchard, D., Rottapel, R., Saito, T. & Penninger, J.M. (2004) The molecular adapter Carma1 controls entry of IκB kinase into the central immune synapse. *J. Exp. Med.* **200**, 167–177.

Hashimoto, A., Takeda, K., Inaba, M., Sekimata, M., Kaisho, T., Ikehara, S., Homma, Y., Akira, S. & Kurosaki, T. (2000) Cutting edge: essential role of phospholipase C-γ2 in B cell development and function. *J. Immunol.* **165**, 1738–1742.

Horwood, N.J., Page, T.H., McDaid, J.P., Palmer, C.D., Campbell, J., Mahon, T., Brennan, F.M., Webster, D. & Foxwell, B.M. (2006) Bruton's tyrosine kinase is required for TLR2 and TLR4-induced TNF, but not IL-6, production. *J. Immunol.* **176**, 3635–3641.

Jefferies, C.A., Doyle, S., Brunner, C., Dunne, A., Brint, E., Wietek, C., Walch, E., Wirth, T. & O'Neill, L.A. (2003) Bruton's tyrosine kinase is a Toll/interleukin-1 receptor domain-binding protein that participates in nuclear factor κB activation by Toll-like receptor 4. *J. Biol. Chem.* **278**, 26258–26264.

Kim, Y., Moon, J.S., Lee, K.S., Park, S.Y., Cheong, J., Kang, H.S., Lee, H.Y. & Kim, H.D. (2004) Ca^{2+}/calmodulin-dependent protein phosphatase calcineurin mediates the expression of iNOS through IKK and NF-κB activity in LPS-stimulated mouse peritoneal macrophages and RAW 264.7 cells. *Biochem. Biophys. Res. Commun.* **314**, 695–703.

Kimura, A., Kinjyo, I., Matsumura, Y., Mori, H., Mashima, R., Harada, M., Chien, K.R., Yasukawa, H. & Yoshimura, A. (2004) SOCS3 is a physiological negative regulator for granulopoiesis and granulocyte colony-stimulating factor receptor signaling. *J. Biol. Chem.* **279**, 6905–6910.

Matsumura, Y., Kobayashi, T., Ichiyama, K., Yoshida, R., Hashimoto, M., Takimoto, T., Tanaka, K., Chinen, T., Shichita, T., Wyss-Coray, T., Sato, K. & Yoshimura, A. (2007) Selective expansion of foxp3-positive regulatory T cells and immunosuppression by suppressors of cytokine signaling 3-deficient dendritic cells. *J. Immunol.* **179**, 2170–2179.

McGettrick, A.F., Brint, E.K., Palsson-McDermott, E.M., Rowe, D.C., Golenbock, D.T., Gay, N.J., Fitzgerald, K.A. & O'Neill, L.A. (2006) Trif-related adapter molecule is phosphorylated by PKCε during Toll-like receptor 4 signaling. *Proc. Natl. Acad. Sci. USA* **103**, 9196–9201.

Nishizuka, Y. (1995) Protein kinase C and lipid signaling for sustained cellular responses. *FASEB J.* **9**, 9484–9496.

O'Neill, L.A. & Bowie, A.G. (2007) The family of five: TIR-domain-containing adaptors in Toll-like receptor signalling. *Nat. Rev. Immunol.* **7**, 353–364.

Rogers, N.C., Slack, E.C., Edwards, A.D., Nolte, M.A., Schulz, O., Schweighoffer, E., Williams, D.L., Gordon, S., Tybulewicz, V.L., Brown, G.D. & Reis e Sousa, C. (2005) Syk-dependent cytokine induction by Dectin-1 reveals a novel pattern recognition pathway for C type lectins. *Immunity* **22**, 507–517.

Shapira, L., Sylvia, V.L., Halabi, A., Soskolne, W.A., Van Dyke, T.E., Dean, D.D., Boyan, B.D. & Schwartz, Z. (1997) Bacterial lipopolysaccharide induces early and late activation of protein kinase C in inflammatory macrophages by selective activation of PKC-ε. *Biochem. Biophys. Res. Commun.* **240**, 629–634.

Shinji, H., Akagawa, K.S., Tsuji, M., Maeda, M., Yamada, R., Matsuura, K., Yamamoto, S. & Yoshida, T. (1997) Lipopolysaccharide-induced biphasic inositol 1,4,5-trisphosphate response and tyrosine phosphorylation of 140-kilodalton protein in mouse peritoneal macrophages. *J. Immunol.* **158**, 1370–1376.

Supajatura, V., Ushio, H., Nakao, A., Akira, S., Okumura, K., Ra, C. & Ogawa, H. (2002) Differential responses of mast cell Toll-like receptors 2 and 4 in allergy and innate immunity. *J. Clin. Invest.* **109**, 1351–1359.

Valledor, A.F., Xaus, J., Comalada, M., Soler, C. & Celada, A. (2000) Protein kinase Cε is required for the induction of mitogen-activated protein kinase phosphatase-1 in lipopolysaccharide-stimulated macrophages. *J. Immunol.* **164**, 29–37.

Wang, Y, Wu J, & Wang, Z. (2006) Akt binds to and phosphorylates phospholipase C-γ1 in response to epidermal growth factor. *Mol. Biol. Cell* **17**, 2267–2277.

Zhou, X., Yang, W. & Li, J. (2006) Ca^{2+}- and protein kinase C-dependent signaling pathway for nuclear factor-κB activation, inducible nitric-oxide synthase expression, and tumor necrosis factor-α production in lipopolysaccharide-stimulated rat peritoneal macrophages. *J. Biol. Chem.* **281**, 31337–31347.

Received: 3 September 2007
Accepted: 15 November 2007

Int J Hematol (2008) 88:82–87
DOI 10.1007/s12185-008-0103-6

ORIGINAL ARTICLE

JAK2 V617F mutation is rare in idiopathic erythrocytosis: a difference from polycythemia vera

Kentaro Yoshinaga · Naoki Mori · Yan-hua Wang · Kaori Tomita · Masayuki Shiseki · Toshiko Motoji

Received: 17 March 2008 / Accepted: 26 March 2008 / Published online: 6 June 2008

Abstract A single mutation 1849G>T in the *JAK2* gene (V617F) has recently been described in classical myeloproliferative disorders (MPD). To investigate the incidence and clinical significance of the *JAK2* mutation, we performed allele-specific polymerase chain reaction (PCR) and enzyme-based assessment in 11 idiopathic erythrocytosis (IE) and 15 polycythemia vera (PV) patients. Aberrant bands indicating the V617F mutation were detected in only one of 11 patients with IE, whereas all of the 15 patients with PV showed the *JAK2* mutation. Sequence analysis was subsequently performed in the IE patient showing aberrant bands on allele-specific PCR, and a nucleotide change corresponding to the V617F mutation was detected in four of 29 clones tested. This patient might have progressed to PV according to the new WHO diagnostic criteria proposed in 2007, since a gradual increase in platelet counts was observed 4 years after the time of diagnosis. A further longitudinal study monitoring V617F positive-cells will clarify the process of progression from IE to PV in such a patient.

Keywords JAK2 · Idiopathic erythrocytosis · Polycythemia vera

K. Yoshinaga · N. Mori (✉) · Y. Wang · K. Tomita · M. Shiseki · T. Motoji
Department of Hematology,
Tokyo Women's Medical University,
8-1 Kawada-cho, Shinjuku-ku, Tokyo 162-8666, Japan
e-mail: mori@dh.twmu.ac.jp

1 Introduction

Janus kinase 2 (JAK2) is a tyrosine kinase involved in the cytokine signaling of several growth factors such as erythropoietin and thrombopoietin in normal and neoplastic cells [1]. A single mutation 1849G>T in the *JAK2* gene, which causes the substitution of phenylalanine for valine at position 617 (V617F), has recently been described in classical myeloproliferative disorders (MPD) [2–5]. The *JAK2* mutation has been found in 65–97% of patients with polycythemia vera (PV), and in half of those with essential thrombocythemia (ET) and idiopathic myelofibrosis (IMF). The *JAK2* V617F mutation was located in the pseudokinase domain, which negatively regulates activity of the kinase domain. This mutation causes the constitutive activation of the JAK2 kinase, resulting in the acceleration of cellular proliferation. Detection of the *JAK2* mutation has recently been included in the World Health Organization (WHO) diagnostic criteria for PV [6].

Idiopathic erythrocytosis (IE) is characterized by an increase in red cell mass without an identified cause [7–9]. IE differs from PV by the absence of splenomegaly, granulocytosis, and thrombocytosis. The term "pure erythrocytosis" is considered identical to IE. Najean et al. [10] reported that 10% of 51 patients diagnosed as having pure erythrocytosis at initial presentation, showed progression to PV at the late stage of the clinical course. In addition, Michiels et al. [11] proposed that IE was the first stage of PV. However, the significance of the *JAK2* V617F mutation in patients with IE remains unclear.

To investigate the incidence and clinical significance of the *JAK2* mutation in Japanese patients with IE, we performed allele-specific polymerase chain reaction (PCR) and restriction enzyme-based assessment. We also

analyzed the *JAK2* mutation in PV to elucidate the difference between IE and PV.

2 Materials and methods

2.1 Patients and samples

Peripheral blood or bone marrow samples were obtained from 11 patients with IE and 15 patients with PV. All samples were obtained under written informed consent. Diagnoses of PV were based on the criteria of the Polycythemia Vera Study Group (PVSG) or WHO 2001 [11–13]. IE was diagnosed in patients demonstrating an increased red cell mass without a known cause of secondary polycythemia and various congenital primary erythrocytosis [7–9]. Although, all 11 patients with IE showed a red cell mass over 36 mL/kg in males or 32 mL/kg in females using ^{51}Cr radioisotope, these patients did not fulfill with PV criteria due to the absence of leukocytosis and thrombocytosis at diagnosis. Splenomegaly was absent in all IE patients except one. One patient (IE No. 11) had a slight splenomegaly. The leukemic cell line HEL was used as a positive control and HL-60 was used as a negative control for the *JAK2* V617F mutation.

Neutrophils were purified by dextran sedimentation followed by hypotonic lysis and centrifugation with Ficoll-Conrey (specific gravity 1.077) as previously described by Woodman et al. [14]. Genomic DNA was extracted from neutrophils or leukemic cells using QIAamp DNA blood mini kit (Qiagen, Valencia, CA). In six IE patients, genomic DNA was extracted from smear samples of bone marrow using QIAamp DNA blood micro kit (Qiagen, Valencia, CA).

2.2 Allele-specific PCR analysis of the *JAK2* gene

Allele-specific PCR was performed using primers ALLS-JAK2-R (5′-CTGAATAGTCCTACAGTGTTTTCAGTTTCA-3′), ALLS-JAK2-F (specific) (5′-AGCATTTGGTTTTAAATTATGGAGTATATT-3′), and ALLS-JAK2-IF (internal control) (5′-ATCTATAGTCATGCTGAAAGTAGGAGAAAG-3′) as previously described by Baxter et al. [2]. The ALLS-JAK2-F primer is specific for the mutant allele and contains an intentional mismatch at the third nucleotide from the 3′ end to improve specificity. Each 20 μL of PCR reaction contained 5 μg of DNA template, 2 μL of 10× Buffer, 0.5 U of Taq polymerase (Takara, Ohtsu, Japan), dNTPs and 0.5 μL of each primer. The PCR cycling parameters were the following: one cycle of 94°C for 5 min, 36 cycles of 94°C for 60 s, 58°C for 60 s and 72°C for 60 s; followed by one cycle of 72°C for 5 min. PCR products were analyzed on a 3% agarose gel.

2.3 Restriction enzyme-based assessment of the *JAK2* gene

Amplification and sequencing of exon 14 of the *JAK2* gene was performed as previously described by Baxter et al. [2] using primers JAK2-14F (5′-GGGTTTCCTCAGAACGTTGA-3′) and JAK2-14R (5′-TCATTGCTTTCCTTTTTCACAA-3′). The PCR cycling parameters were the following: one cycle of 94°C for 5 min, 45 cycles of 94°C for 60 s, 57°C for 60 s and 72°C for 60 s; followed by one cycle of 72°C for 5 min. PCR products were purified with QIAquick PCR purification Kit (Qiagen Valencia, CA). After purification, 460-bp PCR products were digested with *Bsa*XI (New England Biolabs, Hitchin, UK) for 4 h at 37°C, and then analyzed on a 2% agarose gel.

2.4 Sequencing of the *JAK2* gene

Besides PCR products covering exon 14, exon 12 was also amplified using primers by Scott et al. [15]. Sequencing was performed in both directions using a MegaBase sequence system (Amersham, Buckingham, UK). PCR products were purified using QIAquick PCR purification Kit and subsequently analyzed by direct sequencing. In some cases, PCR products were also ligated into pGEM-T vector (Promega, Madison, WI). As a template, one of the plasmid clones containing appropriate PCR products was used for the sequencing reaction. In each case, at least three of the plasmid clones were sequenced. When an alteration in sequence was detected, additional clones were subsequently sequenced.

3 Results

Table 1 shows the clinical and laboratory data of the patients diagnosed as IE and PV. Mean patient age was younger in the IE group than in the PV group ($P = 0.01$). There was a greater male predominance in the IE group than in the PV group. MCV in the IE group was significantly larger than that of the PV group ($P = 0.01$), but there was no significant difference in hematocrit between the IE and PV groups. Red cell mass volume was similar between the IE and PV groups. Serum erythropoietin was significantly higher in the IE group than in the PV group ($P = 0.01$). Although all the patients with PV demonstrated splenomegaly, that finding was observed in only one patient with IE (IE No. 11). Bone marrow showed normocellularity in the majority of IE patients, whereas it was hypercellular in PV.

Table 2 shows the clinical and laboratory data of IE patients. Red cell mass volume was increased without a known cause of secondary polycythemia, and leukocyte

Table 1 Clinical and laboratory data at the time of diagnosis

	IE (n = 11)	PV (n = 15)	P value
Age	47 (25–59)	60 (36–70)	0.01
Male:Female	10:1	8:7	
WBC (/μL)	6,100 (4,090–7,500)	11,400 (7,000–19,400)	<0.01
RBC counts ($\times 10^6$/μL)	604 (559–730)	669 (484–812)	0.08
Hb (g/dL)	19.3 (18.5–21.4)	19.2 (18.8–22.3)	0.12
Hematocrit (%)	57.8 (52.6–65.8)	59.7 (47.7–72.5)	0.94
MCV (fL)	96.3 (85.5–100.7)	87.5 (71.4–98.6)	0.01
Platelet counts ($\times 10^4$/μL)	20.2 (14.4–34.0)	49.6 (30.7–90.6)	<0.01
Red cell mass (mL/kg)	42.9 (37.8–56.0)	44.4 (31.9–65.4)	0.39
Serum erythropoietin (mIU/L) (normal range 7.4–35 mIU/mL)	15.6 (8.5–25.7)	9.3 (3.5–13.5)	0.01
Splenomegaly	–[a]	+++	
Bone marrow cellulality	Normocellular[b]	Hypercellular	

Data are presented as the median (range)

[a] Slight splenomegaly was observed in one patient (IE No.11)

[b] One patient showed hypercellular bone marrow (IE No.11)

Table 2 Clinical and laboratory data at the time of the patients were diagnosed as having idiopathic erythrocytosis

Patient No.	Age	Sex	WBC (μL)	Neutro (%)	RBC ($\times 10^4$/μL)	Hct (%)	Plt ($\times 10^4$/μL)	RBC mass (mL/kg)	sEPO (pg/mL)	Splenomegaly	Duration from diagnosis (years)	BM cellularity	JAK2 mutation	
													PB[a]	BM
1	54	M	6,880	52.7	600	57.8	34.0	43.5	10.1	–	6.6	NE	+	NE
2	58	M	5,500	59.1	568	56.2	16.7	39.1	16.9	–	13.3	NE	–	NE
3	30	M	6,500	48.5	604	54.0	26.6	40.0	15.9	–	3.3	NE	–	NE
4	55	M	6,410	55.8	604	60.3	14.4	56.0	13.6	–	6.3	NE	–	NE
5	39	M	5,260	70.4	730	65.8	17.9	44.1	15.6	–	3.6	Normo	–	–
6	51	M	7,500	71.6	559	56.3	20.0	41.4	18.5	–	12.8	Normo	–	–[a]
7	39	M	5,610	59.6	613	60.2	24.1	42.9	17.5	–	4.0	Normo	–	–
8	36	M	6,000	49.0	566	55.3	17.8	43.2	11.4	–	17.6	Normo	–	–
9	25	M	5,430	70.4	615	52.6	23.2	37.8	13.1	–	2.7	NE	–	NE
10	59	F	4,090	39.1	698	65.2	21.5	47.1	25.7	–	8.2	Normo	–	–
11	47	M	7,400	50.0	645	60.4	20.2	38.6	8.5	+	13.6	Hyper	–	–

Neutro neutrophils, *sEPO* serum erythropoietin, *PB* peripheral blood, *BM* bone marrow, *Normo* normocellular, *Hyper* hypercellular, *NE* not examined

[a] The *JAK2* mutation was analyzed after diagnosis

counts and platelet counts were not increased in any of the patients. The duration of follow-up after diagnosis ranged from 2.7 to 17.6 years (median 6.6 years). Frequent periodic phlebotomy was required in all of the 11 patients. The clinical course and hematological data of four representative patients with IE (IE No. 1, 6, 7, and 10) are shown in Fig. 1. Leukocyte and platelet counts remained stable during observation period in all patients except one (IE No. 1). This patient had slightly higher platelet counts than the others at the time of diagnosis, and his platelet counts gradually increased to over 40 × 10^4/μL during observation (Fig. 1a).

We first performed allele-specific PCR of the *JAK2* gene with peripheral neutrophil DNA in the 11 IE and 15 PV. In Fig. 2a, the 203-bp products indicated amplified mutant allele, and the 364-bp products showed an internal control. Aberrant bands were detected in only one of the 11 IE patients (IE No.1). However, the *JAK2* V617F mutation was detected in all PV patients (data not shown). Subsequently, we performed restriction enzyme-based assessment of the

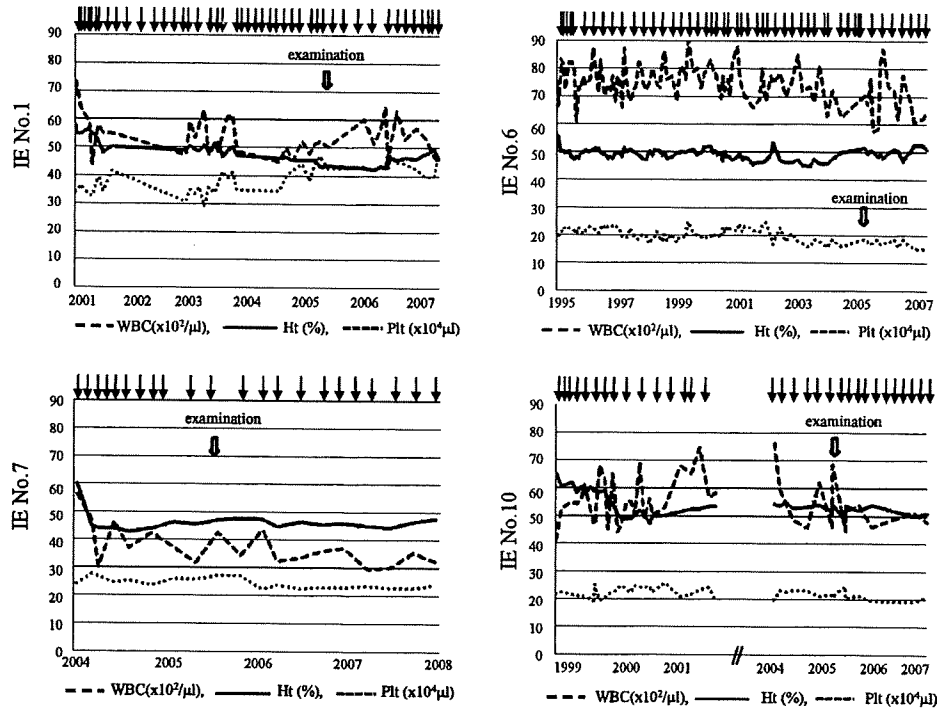

Fig. 1 Clinical course of IE patients. Clinical course and hematological data of four representative patients with IE (IE No. 1, 6, 7 and 10) are shown. *Arrow* indicates phlebotomy. *WBC* white blood cell counts, *Ht* hematocrit, *Plt* platelet cell counts

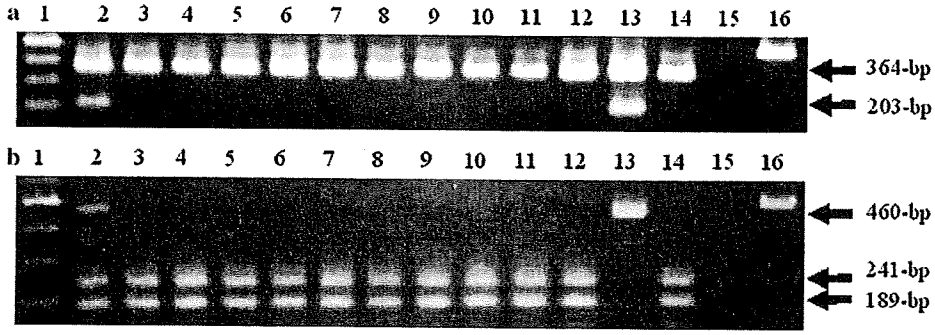

Fig. 2 Allele-specific PCR and restriction enzyme-based assessment of the *JAK2* V617F mutation in IE. **a** Presence of the *lower band* (203-bp product) indicates that the mutation is carried by the patient; the *upper band* (364-bp product) acts as an internal PCR control. *Lane 1* 100-bp marker, lane 2 IE No. 1, lane 3 IE No. 2, *lane 4* IE No. 3, *lane 5* IE No. 4, *lane 6* IE No. 5, *lane 7* IE No. 6, *lane 8* IE No. 7, *lane 9* IE No. 8, *lane 10* IE No. 9, *lane 11* IE No. 10, *lane 12* IE No. 11, *lane 13* HEL, *lane 14* HL–60, *lane 15* water, *lane 16* 500-bp marker. Aberrant bands were observed in only one IE patient (*line* 2, IE No. 1) and positive control (*line 13*, HEL). **b** Restriction enzyme-based assessment of the *JAK2* V617F mutation. Undigested bands (460-bp) were detected in *lane 2* and *lane 13*. The wild type allele was divided to 241-bp, 189-bp and 30-bp fragments. *Lane 1*100-bp marker, *lane 2* IE No. 1, *lane 3* IE No. 2, *lane 4* IE No. 3, *lane 5* IE No. 4, *lane 6* IE No. 5, *lane 7* IE No. 6, *lane 8* IE No. 7, *lane 9* IE No. 8, *lane 10* IE No. 9, *lane 11* IE No. 10, *lane 12* IE No. 11, *lane 13* HEL, *lane 14* HL-60; *lane 15* water, *lane 16* 500-bp marker

V617F mutation (Fig. 2b). The mutant allele was detected as an undigested form (460-bp), whereas the wild type allele was divided into 241, 189, and 30-bp fragments after digestion with *Bsa*XI. The V617F mutation was also detected in one of the 11 patients with IE (IE No.1) and all of the 15 PV patients (Table 2).

We next performed direct sequencing of the samples from 11 IE patients and two PV patients. Representative results are shown in Fig. 3a. The nucleotide change from C to A (reverse direction), corresponding to the *JAK2* V617F mutation, was clearly detected in PV (No. 3) and HEL. By contrast, there was no mutation detected by direct sequencing in samples from ten of the 11 IE patients. In the remaining one IE patient (IE No. 1) with aberrant bands by allele-specific PCR, the nucleotide change was not clearly detected by direct sequencing, but a faint green signal (nucleotide "A") was concurrently observed. To detect a small proportion of the mutation-positive cells, sequence

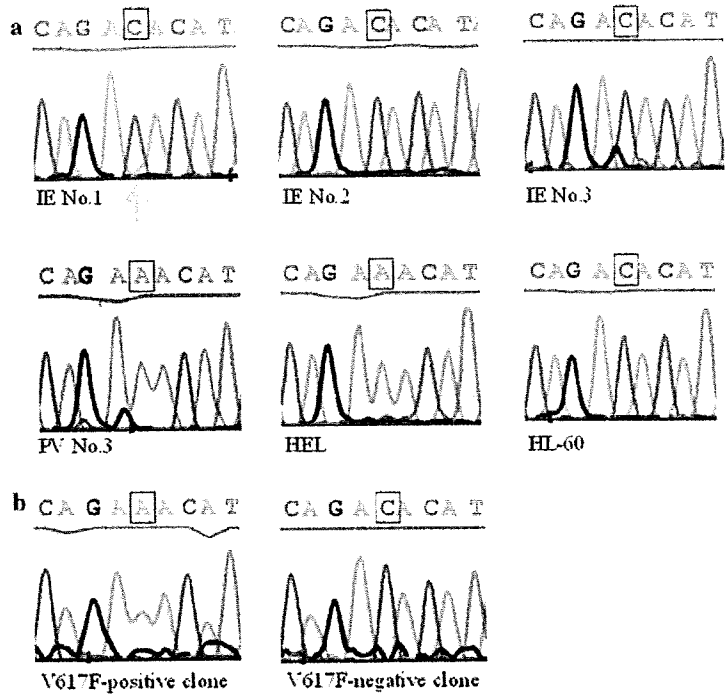

Fig. 3 Sequencing of the *JAK2* gene in erythrocytosis. **a** Direct sequencing was performed in IE, PV and leukemic cell lines. The nucleotide change from C to A (*reverse direction*), corresponding to *JAK2* V617F mutation, was clearly detected in PV No. 3 and HEL. **b** V617F-positive clone is detected in IE No. 1 (*left panel*) and V617F-negative clone is shown in the *right panel*

analysis was performed using plasmid clones containing the *JAK2* gene from IE No. 1. The V617F mutation was detected in four of 29 clones (14.0%) (Fig. 3b).

Since peripheral blood samples do not contain erythroblasts DNA, we used DNA from bone marrow smear samples. However, the *JAK2* V617F mutation was not detectable by allele-specific PCR in bone marrow samples from six IE (Table 2).

To determine the relevance of the *JAK2* mutations other than V617F, we also performed direct sequencing of exon 12. There was no mutation detected in all 11 IE (data not shown).

4 Discussion

The JAK2 V617F mutation was detected in one of the 11 IE patients by allele-specific PCR. The results of restriction enzyme-based assessment were concordant with those of allele-specific PCR. The present results show that the *JAK2* V617F mutation is a rare event in IE. This is apparently different from that of PV, since the *JAK2* V617F mutation was detected in all 15 samples from PV patients in our study. Percy et al. [16] reported that only one of 73 patients with erythrocytosis had the *JAK2* V617F mutation. However, Rossi et al. [17] reported that none of 11 IE had the *JAK2* V617F mutation. Our results indicated that the *JAK2* V617 mutation is rare in IE, differing from the incidence in PV.

In the V617F-positive IE patient, the *JAK2* mutation was subsequently analyzed by sequencing. A small proportion of mutation-positive cells (14.0%) were detected using independent plasmid clones, while the mutation was not clearly observed by direct sequencing. This difference is probably due to the sensitivity of these methods. It is generally considered that the sensitivity of direct sequencing is approximately 10% and that of allele-specific PCR is 2–3%. Proportion of mutation-positive cells of IE No. 1 was much smaller than that of PV. In this patient, his platelet counts were gradually increased over 40 $\times$ $10^4/\mu L$ during observation around the examination (Fig. 1a). This patient might show progression to PV according to the new WHO diagnostic criteria proposed in 2007 [6], although the leukocyte count was within the normal range and splenomegaly was absent. In contrast, none of the remaining ten IE patients (V617F-negative) progressed to PV during long-term observation (median follow up: 6.6 years) from diagnosis to the most recent examination. The absence of the V617F mutation in bone marrow cells suggested that the mutation does not involve the erythroid lineage in these IE patients.

Previous longitudinal studies have reported that patients initially presenting with IE might show hematological evolution and clinical features allowing them to be reclassified as having PV [10, 18–20]. Najean et al. [10] reported that 10% of patients diagnosed as having pure erythrocytosis at initial presentation, progressed to PV at the late stage of the clinical course. In these studies, it was